

A complex network analysis of Spanish river basins

R. Rodríguez-Alarcón

Confederación Hidrográfica del Guadalquivir, Avda. del Brillante, 57, 14012 Córdoba, Spain.

E-mail: rrodriguez@chguadalquivir.es

S. Lozano

Escuela Superior de Ingenieros, University of Seville, Isla de la Cartuja, 41092 Seville, Spain

E-mail: slozano@us.es (corresponding author)

ESTE TRABAJO SE PUBLICÓ EN LA REVISTA

JOURNAL OF HYDROLOGY (2019) vol. 578, 124065

<https://doi.org/10.1016/j.jhydrol.2019.124065>

ABSTRACT

This paper carries out a study of Spanish river basins for the period 2008-2014 using complex network analysis (CNA) tools. The purpose is to gain insight into the structure and characteristics of the national hydrological system with an emphasis on the interconnectivity between the different river basins and the extent to which the current IBT can mitigate the rainfall imbalances of the country, particularly in a scenario of climate change. Apart from the size of the corresponding catchment areas, data on water demand for irrigation, industrial and municipal water supply, historical catchment inflows, reservoir capacity and historical levels, interbasin transfer infrastructures and historical interbasin transfer (IBT) flows, and ocean discharges were collected. A weighted directed network is built with all this information and a number of CNA characterization measures. It has been found that the system has a two-tier structure with a few river basins (hubs) that supply IBT flows to a relatively large number of receiver river basins. Some of those receiver river basins have incoming links from more than one source river basin. This diversification of IBT sourcing is necessary since the availability of water for IBT from a single river basin is not guaranteed. The CNA results also indicate that the IBT infrastructure has been designed to supply water from the river basins with surplus reservoir capacity to river basins with water

30 deficits. The community structure of the system has also been determined with some groups of river
31 basins forming separate, self-sufficient subsystems and other communities minimally connected by IBT
32 links. It can be concluded that the topology and characteristics of the network are a consequence of the
33 imbalances created by the varying climatic conditions of the river basins, the water storage capacity
34 provided by the existing reservoir infrastructure, the geographical and orographic constraints of the
35 country and the high cost of establishing links between neighbouring river basins.

36 **Keywords:** River basins; interbasin transfers; complex network analysis; community structure;
37 assortativity; efficiency

38

39 **1. Introduction**

40 Water is a scarce, strategic natural resource and its effective management has become a necessity and a
41 priority for governments in rich and poor countries alike. Climate change has added pressure and
42 difficulty to this complex task. Water resource management requires balancing supply and demand. The
43 dynamic and uncertain character of supply implies that the necessary reservoirs and, sometimes,
44 interbasin transfer (IBT) infrastructure, needs to be developed and integrated within the existing river
45 basins. This requires planning and has significant social, economic and environmental impacts. Emanuel
46 et al. (2015) highlight the importance of the IBT of surface water resources globally and point to the
47 dearth of information on IBT locations and characteristics, both at the regional and global scales. They
48 also provide an insightful and critical assessment on the effectiveness of IBT to mitigate climate-driven
49 water shortages.

50 In this paper, the Spanish river basin system is studied using the paradigm of complex networks analysis
51 (CNA). CNA is a relatively young, multidisciplinary field whose object is the study of the structure and
52 functions of networks. Although networks (and graphs) have been studied by mathematics and
53 operations research for a long time, it has not been until the last part of the past century that researchers
54 noted the presence and importance of a number of features and phenomena that occur in the real-world
55 networks. New concepts such as small world, scale-free networks, clustering, assortativity, preferential
56 attachment, cascading failures, etc. were introduced and proved very useful to characterize and
57 understand better the growth and behaviour of real-world networks. Moreover, the immense power of
58 networks to capture and model relationships between physical objects or between logical entities has led
59 to an explosion in the number of applications of these techniques, including social networks,
60 transportation networks, power grids, logistics networks, trade networks, tourism flows networks,
61 citations networks, business collaboration networks, etc. Newman (2003) and da Fontoura Costa et al.
62 (2011) provide useful introductory papers on the theory and applications, respectively, of these
63 techniques.

64 CNA has also been applied to hydrology for different purposes. In fact, Sivakumar (2015) argues that the
65 ability of the CNA paradigm to model any type of connection represents a generic theory for studying the
66 connections and evolution of hydrologic systems. Sivakumar et al. (2018) present an overview of
67 applications of CNA in hydrology. Thus, for example, CNA has been applied to Water Distribution
68 Networks (WDN). Some of these studies consider undirected unweighted networks while others consider
69 weighted directed networks. The latter requires knowing the network flows' directions and hence the

70 hydraulics of the system, for example, through EPANET (Soldi et al. 2015). Two main research topics
71 studied in these CNA WDN papers are the structural properties and vulnerability (e.g. Yazdani and
72 Jeffrey 2011, 2012, Yazdani et al. 2011, Shuang et al. 2014, 2015) and the segmentation of WDN for
73 creating District Metered Areas (DMA), controlling leakage or for minimizing contamination risks (e.g.
74 Scibetta et al. 2013, Diao et al. 2013, 2014, Giustolisi and Ridolfi 2014a, 2014b, Giustolisi et al. 2015,
75 Ciaponi et al. 2016).

76 CNA has also been used to study streamflow and river runoff time series (e.g. Tang et al. 2010,
77 Sivakumar and Woldemeskel 2014, Halverson and Fleming 2015, Braga et al. 2016, Serinaldi and Kilsby
78 2016, Fang et al. 2017, Han et al. 2018, Lange et al. 2018, Yasmin and Sivakumar 2018). These studies
79 basically aim at streamflow modelling, classification of catchments and predictions in ungauged basins.

80 A third group of CNA applications to hydrology involves rainfall gauging stations (Scarsoglio et al. 2013,
81 Jha et al. 2015, Sivakumar and Woldemeskel 2015, Jha and Sivakumar 2017, Agarwal et al. 2018,
82 Naufan et al. 2018), satellite-based rainfall data (Malik et al. 2012, Boers et al. 2013, 2014, Marwan and
83 Kurths 2015, Ozturk et al. 2018, Sun et al. 2018) or drought severity time series (Konapala and Mishra
84 2017). These applications study the climate dynamics and spatio-temporal rainfall modeling.

85 Finally, and this is the type of applications most closely related to the one presented in this paper, CNA
86 has also been used to study water resource networks, involving both natural and built components. In this
87 type of studies the nodes of the networks are the stream flows, the reservoirs and the water infrastructure
88 elements, including aqueducts, canals and water supply pipelines (e.g. Porse and Lund 2015, 2016). The
89 main purpose of these studies is to visualize and to study the resilience of the corresponding network.

90 This paper uses the CNA methodology to model a national river basin system and its associated IBT
91 infrastructure. To the best of our knowledge a similar study has not been carried out in the literature. The
92 purpose of this research is to gain insight into the structure and properties of the national hydrological
93 system. In particular, we are interested in the interconnectivity between the different river basins and the
94 extent to which the current IBT can mitigate the rainfall imbalances of the country, particularly in a
95 scenario of climate change.

96 The structure of the paper is the following. Section 2 describes the Spanish river basin system. Section 3
97 describes the methods used in this research while Section 4 presents and discusses the results of the study.
98 Finally, Section 5 summarizes and concludes.

99 **2. Description of the Spanish river basin system**

100 Spain has 15 river basins, some of which discharge into the Atlantic Ocean and others into the
101 Mediterranean Sea. As shown in Figure 1, four of them, namely Miño-Sil, Duero, Tajo and Guadiana,
102 extend to Portugal. Except for the existing engineered inter-basin transfer infrastructure, in principle,
103 these river basins can be considered as autonomous systems, managed by the corresponding public body,
104 called “Confederación Hidrográfica”. The hydrological imbalance between different parts of the country,
105 with some areas (mainly in the northern part of the country) showing excess rainfall and the rest (central,
106 south and eastern parts) suffering rainfall deficits, chronic in some cases, has made it necessary to build
107 an IBT infrastructure, managed by central government, which in case of need can decree the transfer of
108 specific amounts of water from one river basin to another. The purpose of these water transfers, which
109 are often met with social and political opposition from the source region, is to alleviate water shortages in
110 the receiving basin.

111 ===== Figure 1 =====

112 Table 1 show some characteristics and time series (for the period 2008-2014) of the different river basins,
113 such as the size of the corresponding catchment area, total water demand (including irrigation, industrial
114 and municipal water supply), catchment inflows, reservoir capacity and levels, inter-basin transfer flows
115 and ocean discharges. Note that there is a large disparity between the river basins in terms of their size as
116 well as in the catchment and transfer inflows they receive.

117 ===== Table 1 =====

118 Table 2 shows the existing IBT infrastructures, indicating the connected drainage basins connected, the
119 link length, the link capacity and the average annual flows during the period 2008-2014. Note that one of
120 these pipelines is bidirectional (i.e. the water can flow from either of the two ends to the other) and
121 another is disused. Also, in some cases, there is more than one pipeline between a given pair of river
122 basins.

123 ===== Table 2 =====

124 Figure 2 shows the total demand faced by each river basin and its three components (irrigation, industrial
 125 use and municipal water supply) for the period 2008-2104. The needs of the river basins with largest
 126 demands are basically for irrigation. The river basins with smaller demands are basically for municipal
 127 water supply.

128 ===== Figure 2 =====

129 3. Methods

130 In this section, the CNA metrics and algorithms used in this study are introduced and explained. The
 131 metrics are of two types: global (i.e. for the whole network) and local (i.e. node-level). The basic global
 132 network measures are its order (i.e. the number of nodes, n), its size (i.e. its number of arcs, m) and its
 133 density (i.e. the fraction of possible arcs that actually exist, ρ) For a weighted directed network like the
 134 one considered in this paper, its density is given by $\rho = \frac{m}{n \cdot (n-1)}$. Other global measures of interest are:

- 135 • Reciprocity (`igraph_reciprocity` function of `igraph` package): This is the probability that the
 136 opposite counterpart of an existing directed edge also exists, i.e. $R = \frac{1}{m} \sum_{i,j} A_{ij} \cdot A_{ji} = \frac{1}{m} \text{Tr}(A^2)$,
 137 where $A = (A_{ij})$ is the binary adjacency matrix whose elements indicate whether each arc (i, j)
 138 exists or not. As its name indicates, this measure reflects the degree of bidirectionality of the
 139 connections. In an undirected network all the connections are bidirectional and the reciprocity is one.
 140 If none of the connections is bidirectional then the reciprocity is zero.
- 141 • Transitivity (`igraph_transitivity_undirected` function of `igraph` package): Similar to
 142 the clustering coefficient, the transitivity measures the probability that two neighbors of a vertex are
 143 connected but it is computed at the global level as the ratio of the triangles and the connected triples
 144 in the graph. This measure considers the network as undirected. The corresponding formula is

$$145 \quad T = \frac{3 \cdot \sum_{h>j>i} A_{ij} A_{ih} A_{jh}}{\sum_{h>j>i} (A_{ij} A_{ih} + A_{ji} A_{jh} + A_{hi} A_{hj})} = \frac{\frac{1}{2} \text{Trace}(A^3)}{\sum_{j>i} (A^2)_{ij}}$$

146 • Centralization index (`igraph_centralization_degree` function of `igraph` package): This is
 147 a measure of the extent to which the network topology resembles that of a star. The star is used as
 148 reference because its hub-spoke topology in which the central node is connected with all other nodes
 149 and these are only connected with the central node. In a star, the central node has $n-1$ connections
 150 and the $n-1$ nodes have just 1 connection. For an undirected network the centralization index is

151 measured as $CI = \frac{\sum_i (k^{max} - k_i)}{(n-1)(n-2)}$, where k_i refers to the degree of each node i (i.e. the number of

152 connections it has) and $k^{max} = \max_i k_i$ is the largest degree in the network. For a directed network,

153 the centralization index can be computed using the in-degree or the out-degree of the nodes,

154 $k_i^{in} = \sum_j A_{ji}$ and $k_i^{out} = \sum_j A_{ij}$, respectively.

155 • Average path length (`igraph_average_path_length` function of `igraph` package): This is the
 156 average geodesic distance between any pair of nodes. The geodesic distance between two nodes
 157 (`igraph_shortest_paths` function of `igraph` package) d_{ij} is the length of the shortest

158 directed path from node i to node j . Therefore, the average path length is $\bar{d} = \frac{1}{n \cdot (n-1)} \cdot \sum_i \sum_{j \neq i} d_{ij}$.

159 Note that if two nodes are not connected then, by convention, their geodesic distance is infinite. In
 160 that case, the average path length can be computed taking into account only between the pair of nodes
 161 that are effectively connected. Note also that in the case of a weighted network the geodesic distance
 162 generally uses the lengths of the arcs given by the arc weights W_{ij} . The lower the average path length,
 163 the easiest and the least costly is going (or moving goods or transferring information) between any
 164 pair of nodes in the network.

165 • Diameter (`igraph_diameter` and `igraph_diameter_dijkstra` functions of `igraph`
 166 package): This is the largest geodesic distance between connected nodes $D = \max_{\{(i,j):d_{ij}<\infty\}} d_{ij}$. It

167 corresponds to the worst case, i.e. geodesic distance between the nodes that are farthest apart.

168 • Network efficiency: This is an alternative to the average path length that does not have any problem
 169 when some pairs of nodes are not connected (and hence their geodesic distance is infinite). Instead of
 170 using the arithmetic average, the network efficiency is computed as the harmonic mean of the

171 geodesic distances, i.e. $\eta = \frac{1}{n \cdot (n-1)} \cdot \sum_i \sum_{j \neq i} d_{ij}^{-1}$. The higher the geodesic distances between the
 172 nodes, the lower the efficiency of the movements (or the flow of goods or of the communications)
 173 over the network.

174 • Assortativity coefficient (`igraph_assortativity` function of `igraph` package): The
 175 assortativity of the network with respect to a certain node attribute is the Pearson correlation
 176 coefficient between the value of that attribute for the two nodes linked by each arc. Thus, if each node
 177 i has an attribute x_i then

$$178 \quad r_x = \frac{\frac{1}{m} \cdot \sum_{\{(i,j):A_{ij}=1\}} x_i x_j - \left(\frac{1}{m} \cdot \sum_{\{(i,j):A_{ij}=1\}} x_i \right) \left(\frac{1}{m} \cdot \sum_{\{(i,j):A_{ij}=1\}} x_j \right)}{\sqrt{\frac{1}{m} \cdot \sum_{\{(i,j):A_{ij}=1\}} x_i^2 - \left(\frac{1}{m} \cdot \sum_{\{(i,j):A_{ij}=1\}} x_i \right)^2} \cdot \sqrt{\frac{1}{m} \cdot \sum_{\{(i,j):A_{ij}=1\}} x_j^2 - \left(\frac{1}{m} \cdot \sum_{\{(i,j):A_{ij}=1\}} x_j \right)^2}}$$

179 This assortativity coefficient measures whether nodes with a large value of the attribute are
 180 connected with nodes that also has a large value of that attribute and nodes with a low value are
 181 connected with nodes with low value. If that is the case, the assortativity coefficient (i.e. the
 182 correlation) is positive and there is assortativity. Conversely, if nodes with a large value of the
 183 attribute are connected with nodes with a low value of the attribute then the correlation is negative
 184 and there is disassortativity.

185 • Degree-degree correlation (`igraph_avg_nearest_neighbor_degree` and
 186 `igraph_assortativity_degree` functions of `igraph` package): When the attribute
 187 considered in the assortativity coefficient above is the node degree then we can measure the
 188 degree-degree correlation between the nodes. When the network is directed then the attribute
 189 considered in each end of the links can be the in- or the out-degree of the corresponding node. The
 190 usual way of measuring this type of directed degree-degree correlations is through the distribution of
 191 the corresponding average nearest neighbor degree. Thus, for example, if at the origin node of a link
 192 we consider its out-degree and at the destination node of the link we consider its in-degree, we would
 193 be testing whether nodes with large out-degree are connected with nodes with large in-degree
 194 (assortativity) or with nodes with low in-degree (disassortativity). To that end, for each node i we

195 compute the average out-degree of the nodes that are connected to i , i.e. $k_{nn,i}^{out,in} = \frac{1}{k_i^{in}} \sum_j A_{ji} k_j^{out}$

196 and we average these values for all the nodes with the same value of the in-degree, i.e.

197 $k_{nn}^{out,in}(k^{in}) = \frac{1}{|\{i : k_i^{in} = k^{in}\}|} \cdot \sum_{\{i : k_i^{in} = k^{in}\}} k_{nn,i}^{out,in}$. Plotting $k_{nn}^{out,in}(k^{in})$ as a function of k^{in} allows

198 detecting the existence of assortativity or disassortativity between those two degree variables
 199 depending on whether the function is increasing or decreasing. If the degree variables whose
 200 correlation we want to compute are the out-degree of the origin node and the out-degree of the
 201 destination node then the procedure is similar and the corresponding mathematical formulae would

202 be $k_{nn,i}^{out,out} = \frac{1}{k_i^{out}} \sum_j A_{ij} k_j^{out}$ and $k_{nn}^{out,out}(k^{out}) = \frac{1}{|\{i : k_i^{out} = k^{out}\}|} \cdot \sum_{\{i : k_i^{out} = k^{out}\}} k_{nn,i}^{out,out}$.

203 As regards the node-level CNA measures, apart from the in- and out-degree already mentioned, the
 204 following indexes can be computed:

205 • Strength (igraph_strength function of igraph package): This is the sum of the weights of the
 206 arcs that leave a node, out-strength, $s_i^{out} = \sum_j W_{ij}$ or of the arcs that enter the node, in-strength

207 $s_i^{in} = \sum_j W_{ji}$

208 • Node out-efficiency: This is the harmonic mean of the geodesic distance from a given node to every
 209 other node in the network, i.e. $\eta_i^{out} = \frac{1}{n-1} \cdot \sum_{j \neq i} d_{ij}^{-1}$. It measures how easy it is to reach any node
 210 from that node. The average of the node out-efficiencies is equal to the network efficiency, i.e.

211 $\eta = \frac{1}{n} \cdot \sum_i \eta_i^{out}$.

212 • Node in-efficiency: This is the harmonic mean of the geodesic distance to a given node from every
 213 other node in the network, i.e. $\eta_i^{in} = \frac{1}{n-1} \cdot \sum_{j \neq i} d_{ji}^{-1}$. It measures how easy it is to reach that node from

214 any node. The average of the node in-efficiencies is also equal to the network efficiency, i.e.

215
$$\eta = \frac{1}{n} \cdot \sum_i \eta_i^{in}.$$

216 • Betweenness centrality (`igraph_betweenness` function of `igraph` package): The normalized
217 betweenness centrality of a node i corresponds to the fraction of shortest paths between each pair of
218 nodes of the network that pass through node i averaged for all such pairs of nodes (that are distinct
219 from i). The unnormalized measure is the sum of the number of shortest path between any pair of

220 nodes that pass through node i , i.e. $\beta_i^{unnormalized} = \sum_{\substack{j \neq p \\ j \neq i \neq p}} \sigma(j, p/i)$ where $\sigma(j, p/i)$ is the

221 number of shortest paths from j to p that pass through i .

222 Although, as indicated above, the in- and out-degree and the in- and out-strength are local measures, their
223 distribution is a global feature. Thus, for example, some complex networks have a scale free topology
224 with a power law degree distribution in which most nodes have a very small degree and a few nodes
225 (called hubs) has a very large degree. In other cases, like in random networks, the degree distribution is
226 more homogeneous, with most node having a degree around the average degree.

227 When not all the nodes in a network are connected then the network can be partitioned into separate
228 components (`igraph_clusters` function of `igraph` package). A component is a connected subgraph
229 (i.e. a subset of nodes so that from each of them one can go to any other) of maximal cardinality (i.e. if a
230 node that belongs to the component has a link with some other node, that other node also belongs to the
231 component). In directed networks one can distinguish between strongly connected components and
232 weakly connected components. The former take into account the direction of the arcs while the latter
233 correspond to the associated undirected network formed ignoring the direction of the arcs.

234 Finally, most real word networks have a community structure and that is also a global feature of the
235 network. A community, also labeled a module, corresponds to a cluster of nodes that have more
236 connections among themselves than with nodes outside the community. There are many methods for
237 community detection in complex networks (see Fortunato 2010 for a survey). Some of those methods,
238 like Clauset et al. (2004), `igraph_community_fastgreedy` function of `igraph` package, or
239 Blondel et al. (2008), `igraph_community_multilevel` function of `igraph` package, are based on
240 the optimization of modularity (Newman 2006). The modularity function, `igraph_modularity`

241 function of igrph package, is a measure that indicates to what extent a given partition of the nodes
 242 represents the actual community structure of the network. Normally, to identify the community structure
 243 an undirected network is considered. Let a_c the number of edges within each community c and b_c the
 244 sum of the degree of all the nodes in community c . Then, the modularity is computed as
 245
$$Q = \sum_c \left[\frac{a_c}{m} - \left(\frac{b_c}{2m} \right)^2 \right]$$
. The first term within the brackets is the fraction of edges that actually fall within
 246 each community while the second represents the expected number that should fall in that community
 247 according to the corresponding null model (i.e. a network with the same number of nodes and edges and
 248 the same degree distribution). The modularity of the partition that has all nodes as a single community is
 249 zero while the modularity of a partition in which each node constitutes a community is negative. The
 250 larger the value of the modularity of a partition, the better that partition matches the actual community
 251 structure of the network. Since the modularity cannot exceed one, a partition with a modularity value
 252 above 0.3 is generally considered a good fit.

253 **4. Results**

254 The Spanish river basin network has 15 nodes and 14 arcs. It is a weighted directed network where the
 255 weights considered depend on the purpose of the analysis. Thus, it can be either the physical length, the
 256 capacity of the transfer link or the transfer flow in a specific year or over the whole period. Table 3
 257 shows some global network characterization measures. Note that there is no transitivity (i.e. there are
 258 no triangles in the network), which is reasonable as this would involve expensive and unnecessary
 259 connections between already connected nodes. There is a small reciprocity, due to the existence of
 260 some bidirectional links. Bidirectional links allow either of the two river basins connected to transfer
 261 water to the other. Almost all links are, however, unidirectional and hence the source and destination of
 262 the transfers are fixed. The network is sparse, i.e. the number of links is relatively small. Recall that
 263 each link involves a significant investment and hence their number is limited. The in-degree
 264 centralization index is very low but the out-degree centralization index is not so. Recall that the
 265 centralization index measures the extent to which the network resembles a star with a central,
 266 well-connected node, surrounded by many nodes that are not directly connected among themselves.
 267 Therefore, the Spanish river basin network shows some similarity with an out star.

268 ===== Table 3 =====

269 The diameter of the network is rather large (498.1 km). This is the largest geodesic distance between any
270 pair of connected nodes. The diameter corresponds to the length of the longest transfer that may be
271 carried out in the network. The average path length, i.e. the average of the geodesic distances (between
272 connected nodes) is 167.3 km. Measured in terms of number of links, i.e. considering the unweighted
273 network, the diameter is 4 and the average path length is 1.67. This means that the longest possible
274 transfer would involve four consecutive IBT links. Table 4 shows the geodesic distances between each
275 pair of nodes. The entries correspond to the unconnected pairs of nodes are left blank. The bold entry is
276 the network diameter, which corresponds to the length of the shortest path between the TAJ and GDQ
277 nodes. That shortest path is shown in red in Figure 3.

278 ===== Table 4 =====

279 ===== Figure 3 =====

280 It can be seen both in Figure 3 and in Table 4 that most pairs of nodes are unconnected. Actually, the
281 network has four weakly connected components, one of them (namely DUE) is a singleton. The other
282 three components are {TAJ, GDN, TOP, GDQ, CMA, GBB, JUC, SEG}, i.e. the river basins in the
283 Centre and South of Spain, {EBR, CIC, COC, COR}, i.e. the river basins in the North and Northeast of
284 Spain, and {GLC, MÑS}, in the Northwest of the country.

285 Figure 4 shows the community structure identified using the fast greedy hierarchical agglomerative
286 algorithm proposed in Clauset et al. (2004). The right panel of the figure shows the dendrogram that
287 summarizes the agglomerative process in which the nodes are progressively merged into larger clusters
288 by greedily maximizing the modularity improvement in each step. The level of the dendrogram that
289 gives the maximum value of modularity ($Q = 0.53$) corresponds to the seven clusters shown on the left
290 panel. Note that two of the river basins, namely DUE and CIC belong to independent, single-node
291 clusters. DUE has no connections with any other river basin. CIC, which lies on the Northeast of Spain,
292 receives transfers just from EBR, which is grouped in a different cluster, together with COR and COC,
293 both on the North of Spain. There is another three-node cluster that groups three river basins to the
294 South, namely GDQ, CMA and GBB. The other river basin on the Southwest of pain, TOP, is clustered
295 with the river basin that feeds it, GDN. The two Eastern reiver basins, JUC and SEG, which are the
296 ones with largest rainfall deficits in the country, are grouped with the river basin that supplies to them,
297 TAJ. It is interesting to note that there is a single arc connecting each of these three communities,

298 indicating that the IBT infrastructure aims at maintaining connectivity at minimum cost. Finally, the
299 two Northwest river basins, GLC and MÑS, form a separate, self-sufficient subsystem. Recall that the
300 Northwest is the Spanish region with the highest precipitation level.

301 ===== Figure 4 =====

302 Figure 5 shows the distribution of the in- and out-degree. It can be seen that, due to the high cost of the
303 links, most nodes have a low in-degree. The out-degree is, however, relatively high for some donor
304 river basins (namely TAJ and EBR), part of whose hydrological surplus can be transferred to other
305 regions. Therefore, the in-degree distribution shows that the river basins receive transfer from one or at
306 most two other basins while the out-degree distribution shows that some river basins with surplus water
307 can transfer it to four other river basins (the out-degree of EBR is five but some of its outgoing links go
308 to the same river basins, CIC and COR).

309 ===== Figure 5 =====

310 Very informative also is the strength distribution. Thus, Figure 6 shows, for the period 2008-2104, the
311 in- and out-strength of the different river basins, in decreasing order. This allows the easy identification
312 of those river basins that receive the largest amounts of water transfers and those that are the largest
313 donors. Note that although EBR has a larger out-degree, it is TAJ that has the largest out-strength.
314 These two river basins, and to a lesser extent GDN and CMA, constitute the main IBT sources. As
315 regards in-strength, the main receivers of IBT flows are SEG, in Eastern part of Spain, followed by
316 COR (in the North) and TOP (in the Southwest). These correspond with the river basins with the largest
317 deficit between catchment inflows and local demand and that is why they require the largest IBT
318 inflows. Note also that some river basins with non-zero in-degree (namely EBR, MÑS, COC and GDQ)
319 have zero in-strength. This means that that the corresponding IBT infrastructure was not used at all
320 during the period 2008-2014.

321 ===== Figure 6 =====

322 As regards degree-degree correlations, Figure 7 shows the average out-degree of linking neighbours
323 versus the in-degree of a node and the average out-degree of linked neighbours versus the out-degree of

324 a node. The positive slope in the first case (left panel) is indicative of assortativity and means that
325 nodes with larger in-degrees receive connections from nodes with higher out-degrees, i.e. the river
326 basins with more incoming IBT links feed from the river basins with more outgoing IBT links. In the
327 second case (right panel), the slope is negative and this disassortativity means that the river basins with
328 more outgoing IBT links feed river basins with low outgoing IBT links. All this suggests that the
329 system has a two-tier structure, with some river basins functioning as IBT sources (that supply multiple
330 basins) and other river basins functioning as IBT receivers (that get IBT flows from more than one
331 source). In this regard, note that although having an in-degree larger than one adds flexibility to the IBT
332 system, it is costly and hence it is justified only when the availability of water for IBT from a single
333 river basin is not guaranteed and hence it is necessary to diversify the IBT sources.

334 ===== Figure 7 =====

335 We can also look at the correlation between linked nodes in terms of some relevant node attributes such
336 as, for example, catchment inflows, IBT inflows, reservoir capacity, volume stored in reservoir and
337 total water demand. In complex network analysis this is called assortative mixing. As shown in Table 1,
338 the reservoir capacity has not changed during the period under study and that the annual demand for
339 each river basin is known on average. Therefore, for these two node attributes a single correlation
340 coefficient for the whole period is computed. For the other river basin attributes the correlation can be
341 computed also for each year. As shown in Table 5, most of the assortativity coefficients are negative,
342 indicating a disassortative mixing. This means that nodes with large demand are often connected with
343 nodes of low demand, nodes of large reservoir capacity are often connected with nodes of low reservoir
344 capacity, nodes with large volume of water stored in reservoirs are connected with nodes with low
345 volume of water stored, and nodes with large IBT inflows are connected with nodes with low IBT
346 inflows. All this indicates that the IBT infrastructure has been designed to supply water from the river
347 basins with surplus reservoir capacity to river basins with water deficits. In the case of catchment
348 inflows there are both negative and positive assortativity coefficients, depending on the year. Most
349 years (all but 2009 and 2010) there was a positive correlation between the catchment inflows of the
350 connected river basins (both facing rainfall shortfall or surplus) while in 2009 and 2010 the correlation
351 between the catchment inflows of each pair of connected river basins was negative (with one of the
352 ends of the connection experiencing more rainfall than the other). In this regard, note that, because of
353 the short-term character of the public perception of the water scarcity problem, the social and political

354 resistance to IBT normally arises when the donor river basin experiences low rainfall and occurs even
355 if the receiving river basin experiences an even more acute water shortage.

356 ===== Table 5 =====

357 Another interesting CNA characterization measure is the network efficiency. In the case of the river
358 basin network under study and using the actual lengths (in km) of the different links, it results a rather
359 low network efficiency (0.0026). This is not surprising given to the high cost of building this type of
360 links, which precludes the existence of many connections and shortcuts between the nodes. Figure 8
361 shows the in- and out-efficiency of the different nodes, in decreasing order, and their average (i.e. the
362 network efficiency). The river basins with the highest in- and out-efficiency coincide and their
363 out-efficiency is slightly larger than their in-efficiency, i.e. their outgoing links are generally shorter
364 than their incoming links. There are some exceptions to this rule, however. Thus, for GDN, CIC, MÑS
365 and DUE their out-efficiency is slightly larger than their in-efficiency.

366 ===== Figure 8 =====

367 Figure 9 shows the unnormalized betweenness centrality of each node versus its in- and out-degrees
368 (left and right panels, respectively). The nodes with the highest betweenness centrality (namely GDQ,
369 TOP and CMA) are located in the Southern part of the country and have an in-degree equal to one or
370 two and an out-degree equal to one. These river basins often lie on the shortest path between two other
371 river basins. This means that the water transferred between those two river basins should go through
372 the river basin with the high betweenness centrality. This implies that the corresponding IBT
373 infrastructure is doubly utilized: by the IBT flows whose destination is the river basin with high
374 betweenness centrality and by the IBT flows that pass through that river basin with a different
375 destination.

376 ===== Figure 9 =====

377 Finally, Figure 10 shows a visualization of the network where the nodes have been placed in the
378 centroid of each river basin. The size of each node is proportional to the average catchment inflows
379 (during the period under study 2008-2014). Thus, larger nodes correspond to river basins with large

380 catchment inflows. The node colour shows the average percentage of utilization of the corresponding
381 reservoir capacity. As regards the arcs, their size is proportional to the average flow transferred while
382 their colour shows the percentage of utilization of the corresponding IBT infrastructure. It can be seen
383 that the largest IBT flows correspond to the TAJ-SEG, EBR-COR, EBR-CIC, GDN-TOP and
384 CMA-GBB links. Of these, the EBR-COR and GDN-TOP are those that make a higher utilization of
385 their IBT capacity. The two river basins which supply the largest IBT flows are TAJ and EBR, with the
386 latter having a higher reservoir capacity utilization. Actually, the fact that TAJ supplies large amounts
387 of IBT flows to many neighbouring river basins in spite of its relatively low level of reservoir
388 utilization generates concerns in the population of that region. It is remarkable that DUE, which has the
389 largest catchments inflows of all Spanish river basins, is an isolated node, unconnected with the rest of
390 the system. This is due to the orography of this mountainous region, which makes it technically and
391 economically unfeasible too build any IBT infrastructure. Note also that the North of Spain has more
392 catchments inflows than the South and the East of the country, which are the driest regions. Most of
393 these river basins have low levels of reservoir capacity utilization. It can also be seen in Figure 10 why,
394 as indicated in Figure 9, TOP, GDQ and CMA have high betweenness centrality, followed by GDN and
395 EBR. The two-tier structure of the system, with EBR and TAJ each acting as centre of an out star with
396 peripheral nodes that in some cases have more than one incoming link, is also perceptible. The different
397 connected components are clearly visible and also, with the help of Figure 4, the different communities
398 that form the two largest components.

399 ===== Figure 10 =====

400 **5. Conclusions**

401 In this paper, CNA tools and concepts have been used to study and visualize the structure and
402 interrelationships of the Spanish river basins and the existing IBT infrastructure. This is a novel
403 approach that provides a holistic perspective of the system and at the same time allows assessing the
404 role and centrality of the different nodes of the network. Thus, a number of network characterization
405 measures can be computed, such as the density, reciprocity, centralization index, average path length
406 and diameter, efficiency, etc. The picture these measures draw is of a sparse network, with low
407 reciprocity, zero transitivity, four components (one of them formed by just a single unconnected node),
408 relatively large average path length and diameter, and low efficiency. Most of these features can be
409 explained by the high cost of establishing links between the nodes. The out-degree distribution is

410 broader (maximum out-degree=5) than the in-degree distribution (maximum in-degree=2), i.e. there are
411 a few river basins (namely, EBR and TAJ) that each supply IBT flows to a relatively large number of
412 receiver river basins while those receiver river basins have incoming links from at most two of these
413 source river basins. The CNA results also indicate that the IBT infrastructure has been designed to
414 supply water from the river basins with surplus reservoir capacity to river basins with water deficits and
415 that the system has a two-tier structure, with some river basins functioning as IBT sources (that supply
416 multiple basins) and other river basins functioning as IBT receivers (that get IBT flows from more than
417 one source). This diversification of IBT sourcing implies that the availability of water for IBT from a
418 single river basin is not guaranteed. A neat community structure involving seven small clusters (of two
419 or three nodes generally) has also been identified. It is interesting to note that in most cases there is a
420 single arc connecting these communities, indicating that the IBT infrastructure aims at maintaining
421 connectivity at minimum cost. The in- and out-strength distributions clearly identify the main source
422 and recipient river basins of the IBT flows. They also show that some river basins with incoming IBT
423 links have not made any use of them during the period under study. The in- and out-efficiency of each
424 node and its contribution to the overall network efficiency have also been determined and the nodes
425 with high betweenness centrality have been identified.

426 In summary, this study has carried out a thorough and insightful analysis of the Spanish river basin
427 system and their IBT interconnections. It can be concluded that the topology and characteristics of the
428 network are a consequence of the imbalances created by the varying climatic conditions of the river
429 basins, the water storage capacity provided by the existing reservoir infrastructure, the geographical
430 and orographic constraints of the country and the high cost of establishing links between neighbouring
431 river basins.

432 As a continuation of this research, a more fine-grained study considering the different sub-drainage
433 basins that form each drainage basin is planned. Also, a similar study on a larger scale (e.g. the
434 European river basins) would be desirable. In this regard, it is anticipated that the largest difficulty that
435 would be faced is that of data collection.

436

Acknowledgements

437 This research was carried out with the financial support of the Spanish Ministry of Science and the
438 European Regional Development Fund (ERDF), grant DPI2017-85343-P. The authors would like to
439 thank the associate editor and two anonymous reviewers for their constructive and helpful comments
440 and suggestions.

References

- 442 Agarwal, A., Marwan, N., Maheswaran, R., Merza, B. and Kurths, J., “Quantifying the roles of single
443 stations within homogeneous regions using complex network analysis”, *Journal of Hydrology*, 563
444 (2018) 802-810
- 445 Blondel, V.D., Guillaume, J.L., Lambiotte, R. and Lefebvre, E., “Fast unfolding of communities in
446 large networks”, *Journal of Statistical Mechanics: Theory and Experiment*, 10 (2008) P10008
- 447 Boers, N., Bookhagen, B., Marwan, N., Kurths, J. and Marengo, J., “Complex networks identify spatial
448 patterns of extreme rainfall events of the South American Monsoon System”, *Geophysical Research*
449 *Letters*, 40 (2013) 4386-4392
- 450 Boers, N., Rheinwalt, A., Bookhagen, B., Barbosa, H.M.J., Marwan, N., Marengo, J. and Kurths, J.,
451 “The South American rainfall dipole: A complex network analysis of extreme events”, *Geophysical*
452 *Research Letters*, 41 (2014) 7397-7405
- 453 Braga, A.C., Alves, L.G.A., Costa, L.S., Ribeiro, A.A., de Jesus, M.M.A., Tateishi, A.A. and Ribeiro,
454 H.V., “Characterization of river flow fluctuations via horizontal visibility graphs”, *Physica A:*
455 *Statistical Mechanics and its Applications*, 444 (2016) 1003-1011
- 456 Ciaponi, C., Murari E. and Todeschini, S., “Modularity-Based Procedure for Partitioning Water
457 Distribution Systems into Independent Districts”, *Water Resources Management*, 30 (2016) 2021-2036
- 458 Clauset, A., Newman, M.E.J. and Moore, C., “Finding community structure in very large networks”,
459 *Physical Review E*, 70 (2004) 066111
- 460 da Fontoura Costa, L., Oliveira Jr, O.N., Travieso, G., Rodrigues, F.A., Ribeiro Villas Boas, P.,
461 Antiqueira, L., Palhares Viana, M. and Correa Rocha, L.E., “Analyzing and modeling real-world
462 phenomena with complex networks: a survey of applications”, *Advances in Physics*, 60, (2011)
463 329-412
- 464 Diao, K., Zhou, Y. and Rauch, W., “Automated Creation of District Metered Area Boundaries in Water
465 Distribution Systems”, *Journal of Water Resources Planning and Management*, 139, 2 (2013) 184-190
- 466 Diao, K., Farmani, R., Fu, G., Astaraie-Imani, M., Ward S. and Butler, D., “Clustering analysis of water
467 distribution systems: identifying critical components and community impacts”, *Water Science &*
468 *Technology*, 70, 11 (2014) 1764-1773
- 469 Emanuel, R.E., Buckley, J.J., Caldwell, P.V., McNulty, S.G. and Sun, G., “Influence of basin
470 characteristics on the effectiveness and downstream reach of interbasin water transfers: displacing a
471 problem”, *Environmental Research Letters*, 10 (2015) 124005

472 Fang, K., Sivakumar, B. and Woldemeskel, F.M., “Complex networks, community structure, and
473 catchment classification in a large-scale river basin”, *Journal of Hydrology*, 545 (2017) 478-493

474 Fortunato, S., “Community detection in graphs”, *Physics Reports*, 486 (2010) 75-174

475 Giustolisi, O. and Ridolfi, L., “New Modularity-Based Approach to Segmentation of Water Distribution
476 Networks”, *Journal of Hydraulic Engineering*, 140, 10 (2014a) 04014049

477 Giustolisi, O. and Ridolfi, L., “A novel infrastructure modularity index for the segmentation of water
478 distribution networks”, *Water Resources Research*, 50 (2014b) 7648-7661

479 Giustolisi, O., Ridolfi, L. and Berardi, L., “General metrics for segmenting infrastructure networks”,
480 *Journal of Hydroinformatics*, 17, 4 (2015) 505-517

481 Halverson, M.J. and Fleming, S.W., “Complex network theory, streamflow, and hydrometric
482 monitoring system design”, *Hydrology and Earth System Sciences*, 19 (2015) 3301-3318

483 Han, X., Sivakumar, B., Woldmeskel, F.M. and Guerra de Aguilar, M., “Temporal dynamics of
484 streamflow: application of complex networks”, *Geoscience Letters*, 5:10 (2018)

485 Jha, S.K., Zhao, H., Woldemeskel, F.M. and Sivakumar, B., “Network theory and spatial rainfall
486 connections: an interpretation”, *Journal of Hydrology*, 527 (2015) 13-19

487 Jha, S.K. and Sivakumar, B., “Complex networks for rainfall modeling: spatial connections, temporal
488 scale, and network size”, *Journal of Hydrology*, 554 (2017) 482-489

489 Konapala, G. and Mishra, A., “Review of complex networks application in hydroclimatic extremes with
490 an implementation to characterize spatio-temporal drought propagation in continental USA”, *Journal of*
491 *Hydrology*, 555 (2017) 600-620

492 Lange, H., Sippel, S. and Rosso, O.A., “Nonlinear dynamics of river runoff elucidated by horizontal
493 visibility graphs”, *Chaos*, 28 (2018) 075520

494 Malik, N., Bookhagen, B., Marwan, N. and Kurths, J., “Analysis of spatial and temporal extreme
495 monsoonal rainfall over South Asia using complex networks”, *Climate Dynamics*, 39 (2012) 971-987

496 Marwan, N. and Kurths, J., “Complex network based techniques to identify extreme events and
497 (sudden) transitions in spatio-temporal systems”, *Chaos*, 25 (2015) 097609

498 Naufan, I., Sivakumar, B., Woldemeskel, F.M., Raghavan, S.V., Vu, M.T. and Liong, S.Y., “Spatial
499 connections in regional climate model rainfall outputs at different temporal scales: Application of
500 network theory”, *Journal of Hydrology*, 556 (2018) 1232-1243

501 Newman, M.E.J., “The Structure and Function of Complex Networks”, *SIAM Review*, 45, 2 (2003)
502 167-256

503 Newman, M.E.J., “Modularity and community structure in networks”, *Proceedings of the National*
504 *Academy of Sciences*, 103 (2006) 8577-8582

505 Ozturk, U., Marwan, N., Korup, O., Saito, H., Agarwal, A., Grossman, M.J., Zaiki, M. and Kurths, J.,
506 “Complex networks for tracking extreme rainfall during typhoons”, *Chaos*, 28 (2018) 075301

507 Porse, E. and Lund, J., “Network structure, complexity, and adaptation in water resource systems”,
508 *Civil Engineering and Environmental Systems*, 32, 1-2 (2015) 143-156

509 Porse, E. and Lund, J., “Network Analysis and Visualizations of Water Resources Infrastructure in
510 California: Linking Connectivity and Resilience”, *Journal of Water Resources Planning and
511 Management*, 142, 1 (2016) 04015041

512 Scarsoglio, S., Laio, F. and Ridolfi, L., “Climate Dynamics: A Network-Based Approach for the
513 Analysis of Global Precipitation”, *PLoS ONE*, 8, 8 (2013) e71129

514 Scibetta, M., Boano, F., Revelli, R. and Ridolfi, L., "Community detection as a tool for complex pipe
515 network clustering", *EPL*, 103 (2013) 48001

516 Serinaldi, F. and Kilsby, C.G., “Irreversibility and complex network behavior of stream flow
517 fluctuations”, *Physica A: Statistical Mechanics and its Applications*, 450 (2016) 585-600

518 Shuang, Q., Zhang, M. and Yuan, Y., “Node vulnerability of water distribution networks under
519 cascading failures”, *Reliability Engineering and System Safety*, 124 (2014) 132-141

520 Shuang, Q., Yuan, Y., Zhang, M. and Liu, Y., “A Cascade-Based Emergency Model for Water
521 Distribution Network”, *Mathematical Problems in Engineering*, 2015 (2015) 827816

522 Sivakumar, B., “Networks: a generic theory for hydrology?”, *Stochastic Environmental Research and
523 Risk Assessment*, 29, 3 (2015) 761-771

524 Sivakumar, B. and Woldemeskel, F.M., “Complex networks for streamflow dynamics”, *Hydrology and
525 Earth System Sciences*, 18, 11 (2014) 4565-4578

526 Sivakumar, B. and Woldemeskel, F.M., “A network-based analysis of spatial rainfall connections”,
527 *Environmental Modelling & Software*, 69 (2015) 55-62

528 Sivakumar, B., Puente, C.E. and Maskey, M.L., “Complex Networks and Hydrologic Applications”, in:
529 Tsonis, A.A. (Ed.), *Advances in Nonlinear Geosciences*, Springer, Cham (2018) 565-586

530 Soldi, D., Candelieri, A. and Archetti, F., “Resilience and vulnerability in urban water distribution
531 networks through network theory and hydraulic simulation”, *Procedia Engineering*, 119 (2015)
532 1259-1268

533 Sun, A.Y., Xia, Y., Caldwell, T.G. and Hao, Z., “Patterns of precipitation and soil moisture extremes in
534 Texas, US: A complex network analysis”, *Advances in Water Resources*, 112 (2018) 203-213

535 Tang, Q., Liu, J. and Liu, H., “Comparison of different daily streamflow series in US and China, under
536 a viewpoint of complex networks”, *Modern Physics Letters B*, 24, 14 (2010) 1541–1547

537 Yasmin, N. and Sivakumar, B., “Temporal streamflow analysis: Coupling nonlinear dynamics with
538 complex networks”, *Journal of Hydrology*, 564 (2018) 59-67

539 Yazdani, A. and Jeffrey, P., “Complex network analysis of water distribution systems”, *Chaos*, 21, 1
540 (2011) 016111

541 Yazdani, A., Otto, R.A. and Jeffrey, P., “Resilience enhancing expansion strategies for water
542 distribution systems: A network theory approach”, *Environmental Modelling & Software*, 26 (2011)
543 1574-1582

544 Yazdani, A. and Jeffrey, P., “Water distribution system vulnerability analysis using weighted and
545 directed network models”, *Water Resources Research*, 48 (2012) W06517

546

547 **List of figures and table captions**

548 Figure 1. Spanish river basins

549 Figure 2. Volume and composition of river basin demands (2008-2014)

550 Figure 3. Shortest path between TAJ and GDQ nodes (its length corresponds to the network diameter)

551 Figure 4. Community structure (fast greedy algorithm)

552 Figure 5. In- and out-degree distribution

553 Figure 6. In- and out-strength distribution (average 2008-2014)

554 Figure 7. Degree-degree correlations

555 Figure 8. Network and node in- and out-efficiency

556 Figure 9. Betweenness centrality versus in- and out-degree

557 Figure 10. Visualization of the network. Node size proportional to average catchment inflows. Node
558 colour shows average reservoir capacity utilization. Arc width proportional to average IBT flow. Arc
559 colour shows IBT capacity utilization.

560

561

562

563 Table 1. Basic data of Spanish river basins

564 Table 2. Data on existing inter-basin transfer infrastructure

565 Table 3. Some network characterization measures

566 Table 4. Geodesic distances (km) between nodes (network diameter shown in bold)

567 Table 5. Assortative coefficient for some relevant node attributes

568

569

570

571

572

573



574

575

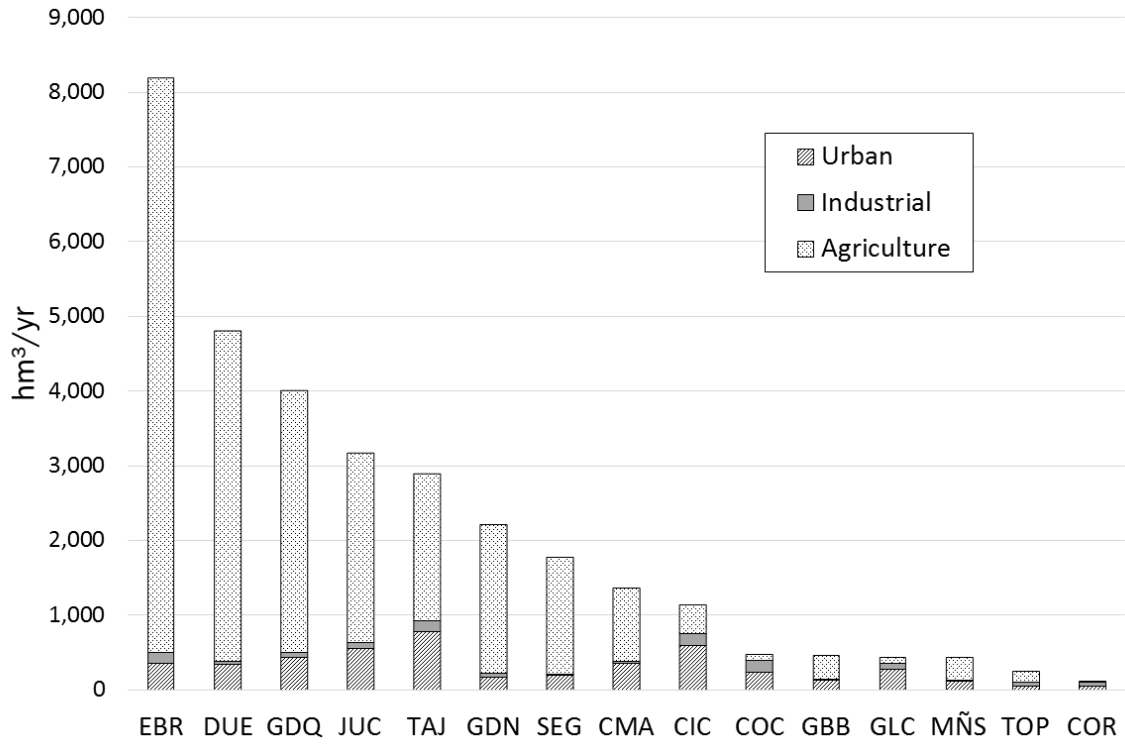
Figure 1. Spanish river basins

576

577

578

579



580

Figure 2. Volume and composition of river basin demands (2008-2014)

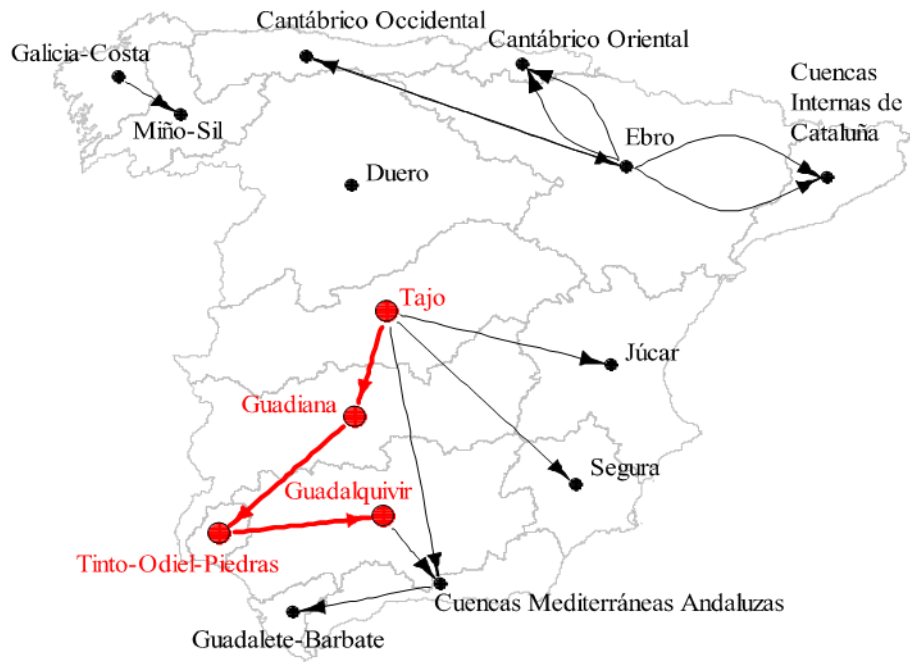
581

582

583

584

585



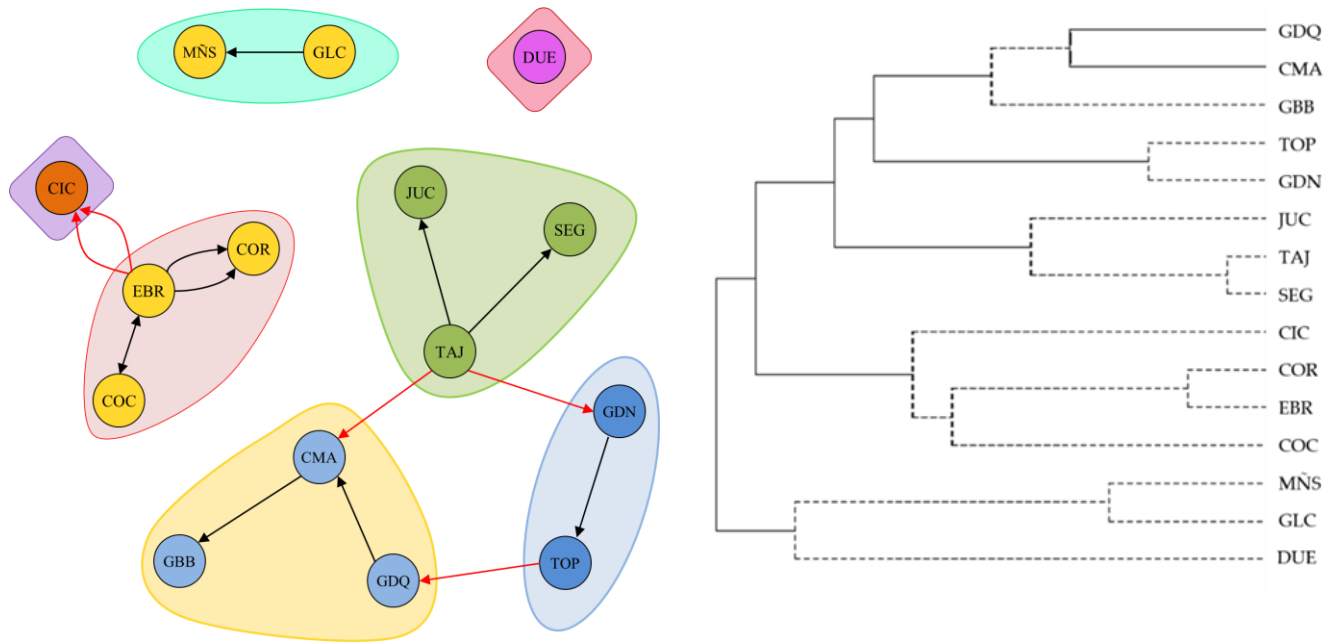
586 Figure 3. Shortest path between TAJ and GDQ nodes (its length corresponds to the network diameter)

587

588

589

590



591

Figure 4. Community structure (fast greedy algorithm)

592

593

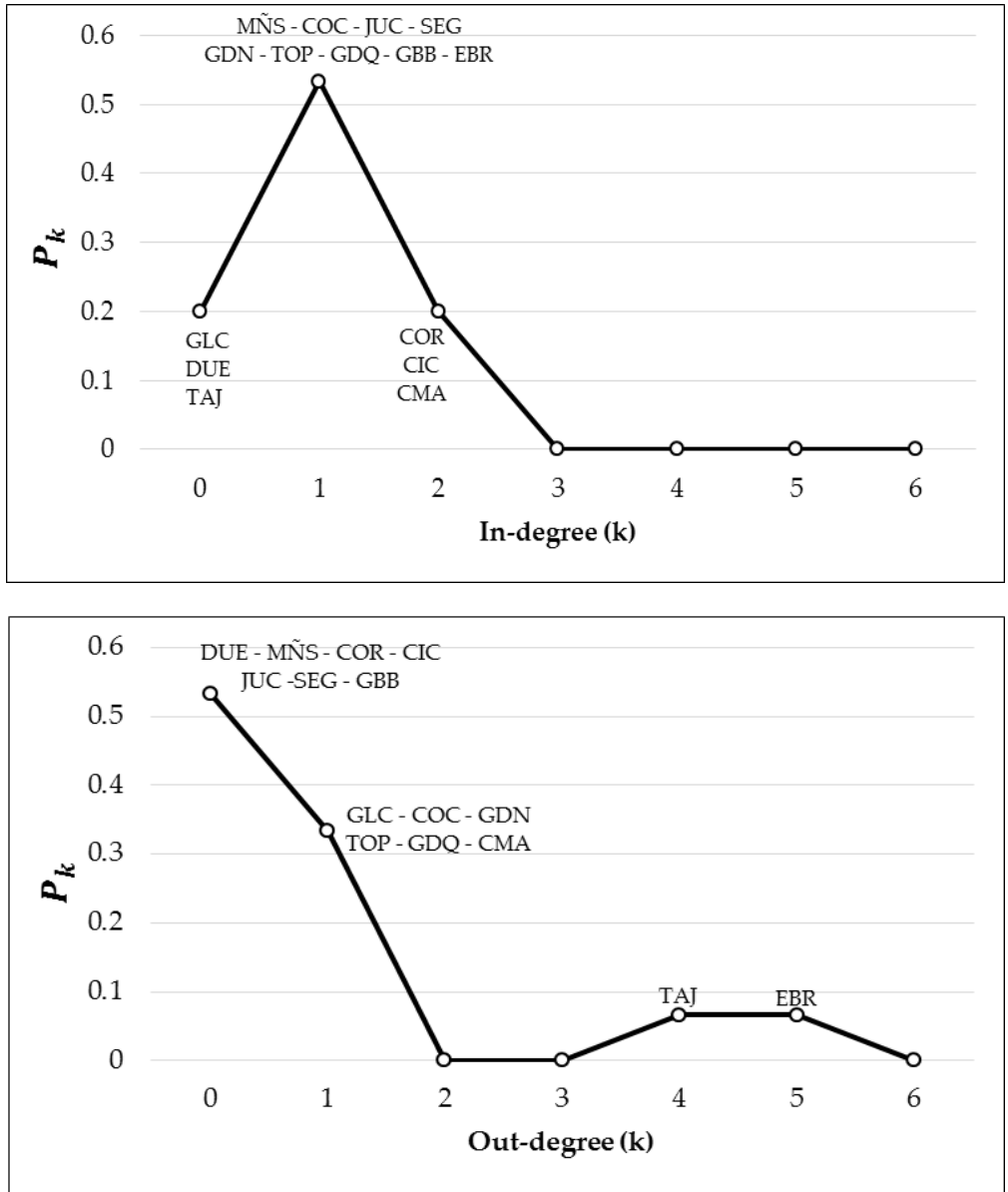
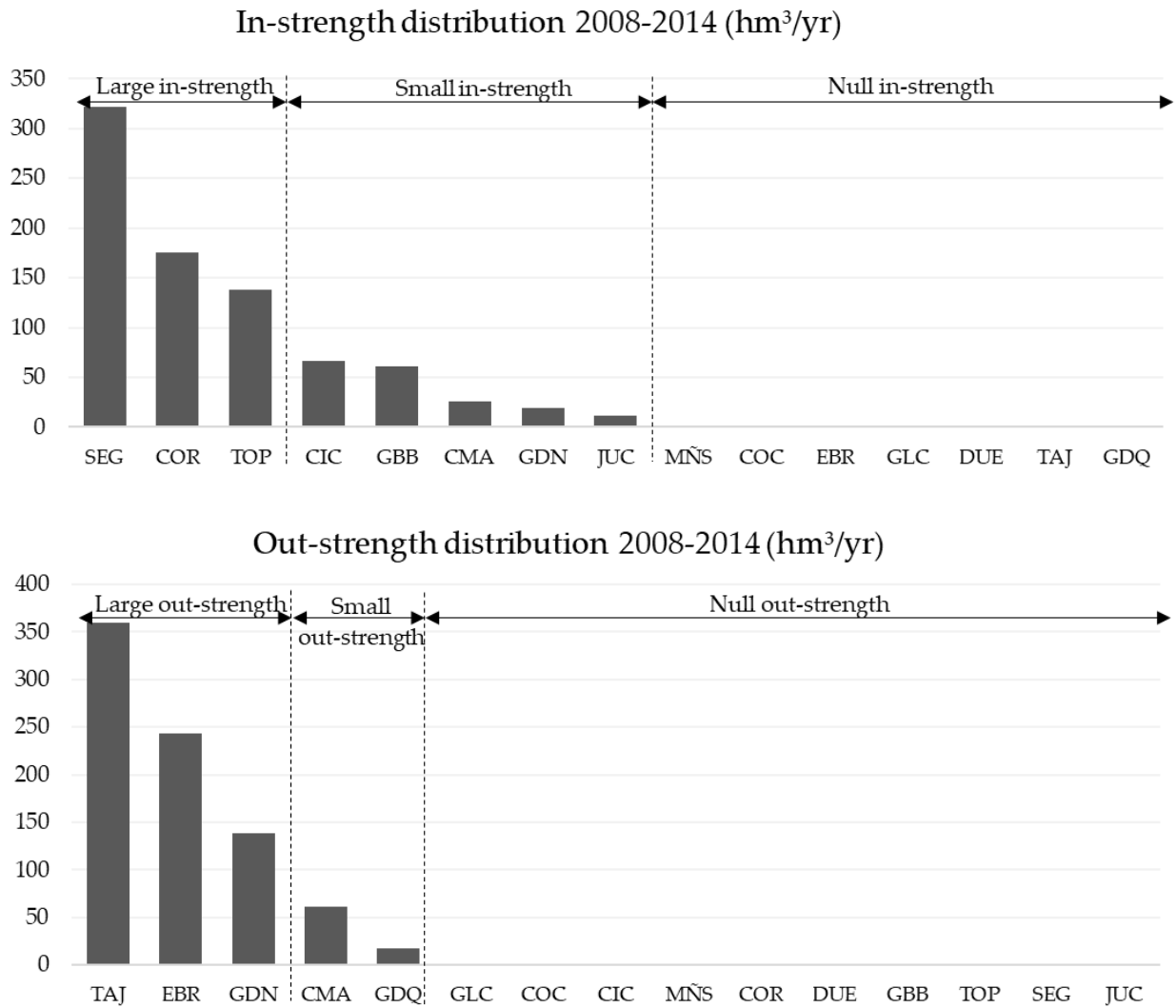


Figure 5. In- and out-degree distribution

599

600



601

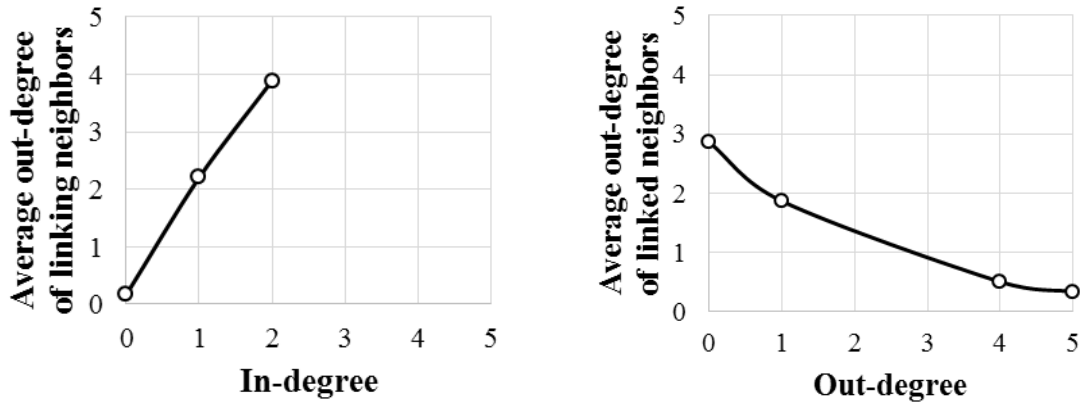
Figure 6. In- and out-strength distribution (average 2008-2014)

602

603

604

605



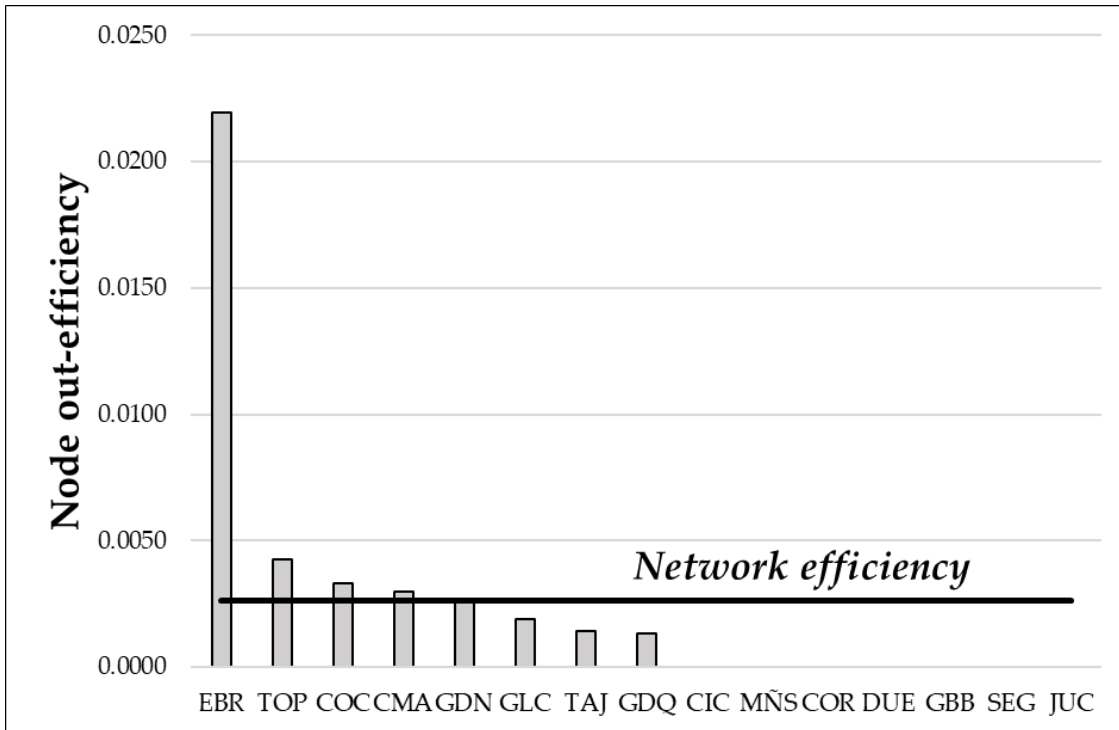
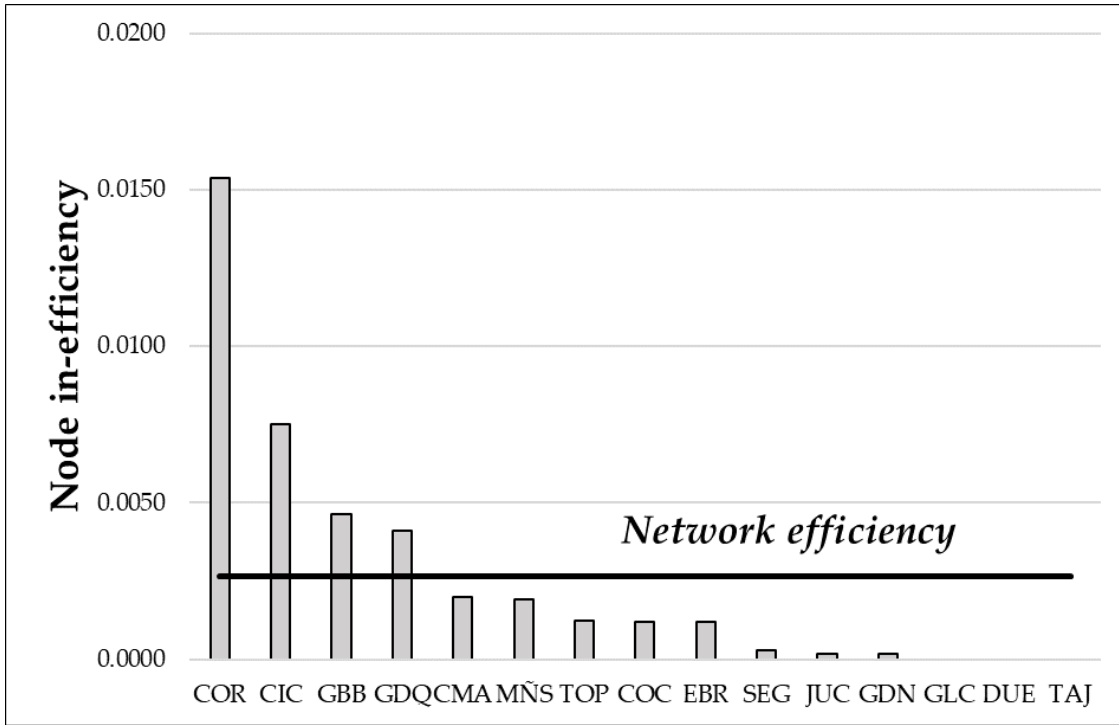
606

Figure 7. Degree-degree correlations

607

608

609



611

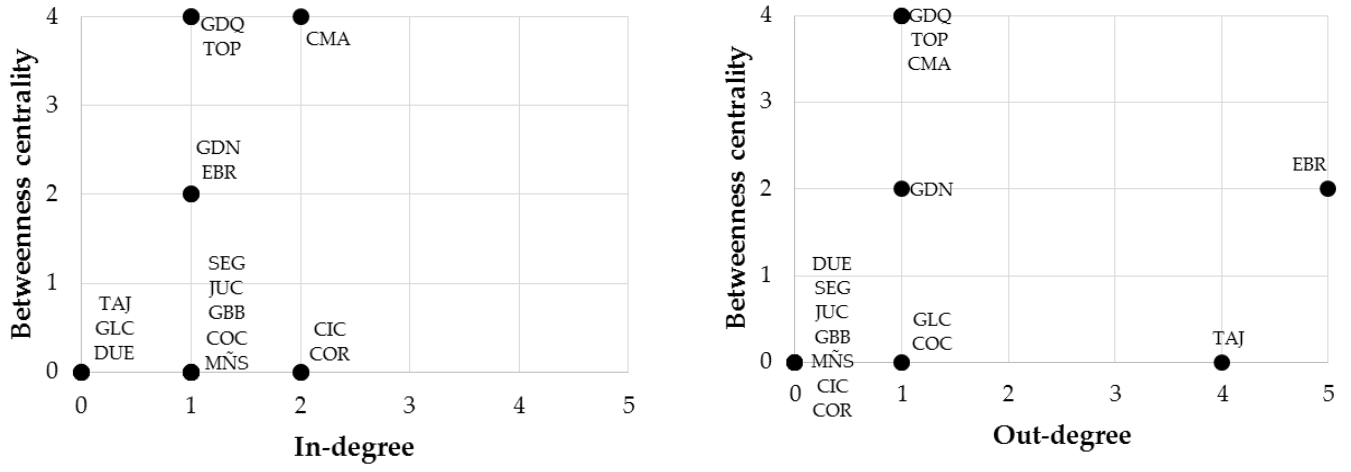
Figure 8. Network and node in- and out-efficiency

612

613

614

615



616

Figure 9. Betweenness centrality versus in- and out-degree

617

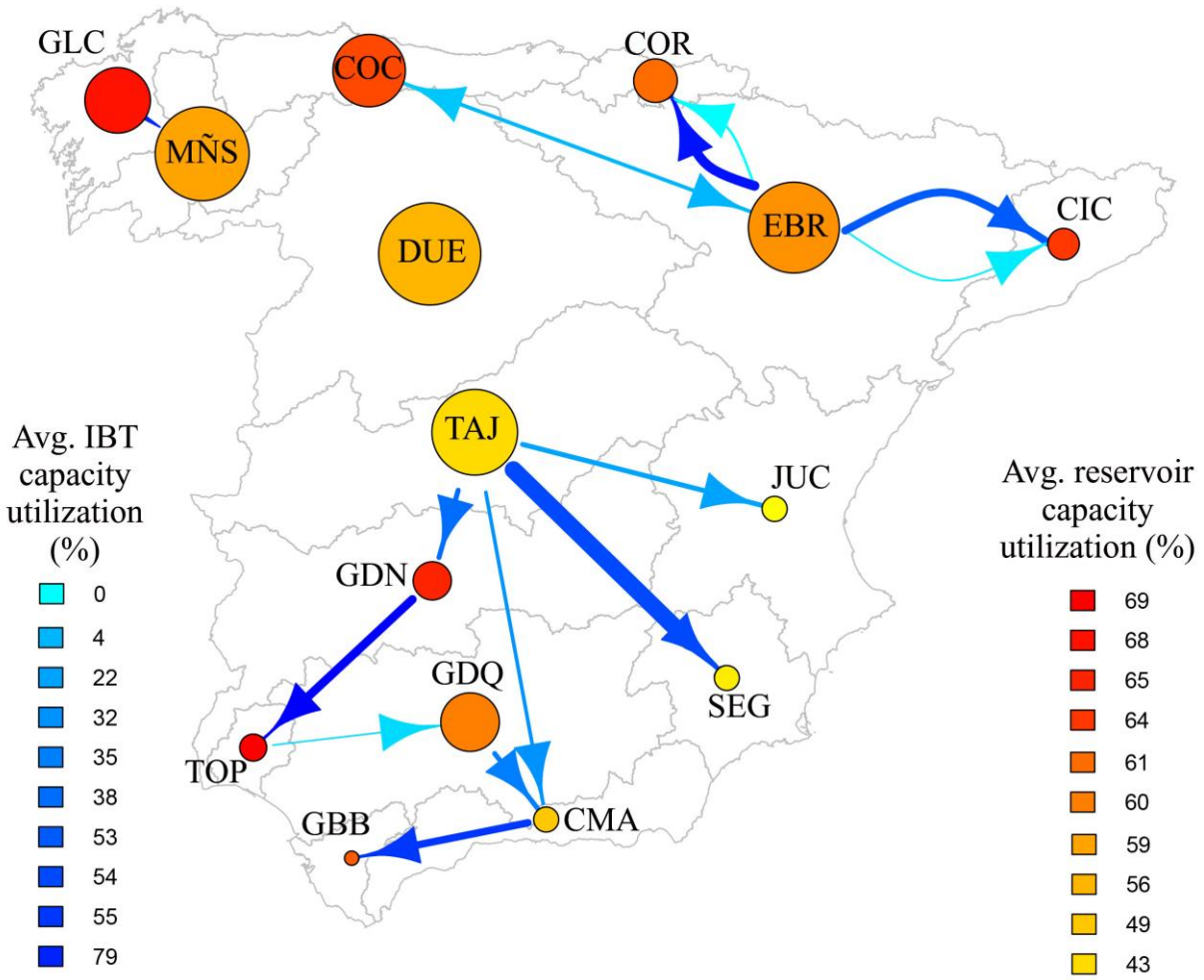
618

619

620

621

622



623

624 Figure 10. Visualization of the network. Node size proportional to average catchment inflows. Node
625 colour shows average reservoir capacity utilization. Arc width proportional to average IBT flow. Arc
626 colour shows IBT capacity utilization.

627

628

629

Table 1. Basic data of Spanish river basins

#	River basin	Label	Catchment area (km ²)	Reservoir capacity (hm ³)	2008-2014				
					Average annual catchment inflows (hm ³)	Average annual transfer inflows (hm ³)	Average annual discharges to ocean (hm ³)	Average annual demand	Average volume stored in reservoirs (hm ³)
1	Cuencas Internas de Cataluña	CIC	16,495.43	740.00	1,162.75	66.54	898.66	1,046.40	514.86
2	Miño.Sil	MÑS	17,603.37	3,030.00	10,733.26	1.58	12,721.47	436.02	1,695.29
3	Galicia.Costa	GLC	13,079.92	684.00	6,112.31	0.00	5,221.04	434.92	388.71
4	Cantábrico Oriental	COR	5,783.90	79.00	2,314.36	175.56	1,118.01	273.03	50.86
5	Cantábrico Occidental	COC	17,417.20	554.00	6,393.38	0.95	8,084.39	769.00	325.86
6	Duero	DUE	78,889.78	7,507.00	12,700.55	0.00	8,680.15	4,800.00	4,194.00
7	Tajo	TAJ	55,780.76	11,012.00	8,940.42	0.00	6,085.06	2,800.02	5,361.71
8	Guadiana	GDN	55,512.10	9,266.00	2,514.89	18.75	815.54	2,217.13	5,914.57
9	Guadalquivir	GDQ	57,187.61	8,101.00	4,184.71	0.00	1,988.30	4,007.73	5,242.71
10	Cuencas Mediterráneas Andaluzas	CMA	17,941.97	1,177.00	1,063.29	17.28	1,085.54	1,392.60	682.29
11	Guadalete.Barbate	GBB	5,956.26	1,651.00	333.11	500.87	NA	438.25	1,139.00
12	Tinto.Odiel.Piedras	TOP	4,762.34	229.00	861.47	138.53	1,000.00	264.68	165.86
13	Segura	SEG	19,024.80	1,141.00	728.67	321.54	7.96	1,722.50	568.57
14	Júcar	JUC	42,729.38	3,330.00	743.90	11.16	453.88	3,240.81	1,358.00
15	Ebro	EBR	85,562.79	7,511.00	10,060.26	1.67	11,063.40	8,385.99	4,038.00

Table 2. Data on existing inter-basin transfer infrastructure

Name	Source basin	Receiving basin	Length (km)	Maximum flow rate (l/s)	Transfer capacity (hm ³ /y)	Average annual transfer volume (hm ³)	Remarks
Ebro – Besaya	EBR	COC	60.00	4,000	27	0.95	Bidirectional
Cernejá – Ordunte	EBR	COR	5.00	160	13	0.00	-
Zadorra – Arratia	EBR	COR	45.39	9,000	190	175.56	-
Ebro–Tarragona	EBR	CIC	97.94	NA	126	66.54	-
Ciurana – Ruidecañas	EBR	CIC	11.00	NA	7	0.00	Disused
Tajo – Segura	TAJ	SEG	248.72	NA	600	321.54	-
Tajo – Segura – Júcar	TAJ	JUC	381,28	NA	NA	11.16	-
Tajo – Segura – Guadiana	TAJ	GDN	408.63	NA	50	18.75	-
Tajo – Segura – CMA	TAJ	CMA	297.58	NA	27	8.67	-
Guadiana – TOP	GDN	TOP	67.00	NA	75	138.53	-
Eiras – Porriño	GLC	MÑS	37.38	NA	NA	1.58	-
TOP – Guadalquivir	TOP	GDQ	22.48	NA	5	0.00	-
Guadiaro – Majaceite	CMA	GBB	24.01	30,000	110	60.76	-
Negratín – Almanzora	GDQ	CMA	96.00	NA	50	17.28	-

Table 3. Some network characterization measures

Nodes	15
Arcs	14
Transitivity	0.00
Reciprocity	0.13
Density	0.067
Centralization index (in-degree)	0.071
Centralization index (out-degree)	0.286
Average path length (unweighted)	1.67
Diameter (unweighted)	4
Average path length (km)	167.33
Diameter (km)	498.11

Table 4. Geodesic distances (km) between nodes (network diameter shown in bold)

To From	CIC	MÑS	GLC	COR	COC	DUE	TAJ	GDN	GDQ	CMA	GBB	TOP	SEG	JUC	EBR
CIC															
MÑS															
GLC		37.38													
COR															
COC	71.00			65.00											60.00
DUE															
TAJ								408.63	498.11	297.58	321.59	475.63	248.72	381.28	
GDN									89.48	185.48	209.49	67.00			
GDQ										96.00	120.01				
CMA											24.01				
GBB															
TOP									22.48	118.48	142.49				
SEG															
JUC															
EBR	11.00			5.00	60.00										

Table 5. Assortative coefficient for some relevant node attributes

Period	Catchment inflows	IBT inflows	Volume stored in reservoirs	Reservoir capacity	Total demand
2008	0.185	-0.136	-0.586	-	-
2009	-0.396	-0.179	-0.352	-	-
2010	-0.428	-0.209	-0.209	-	-
2011	0.419	-0.201	-0.245	-	-
2012	0.072	0.006	-0.471	-	-
2013	0.123	-0.038	-0.443	-	-
2014	0.118	-0.040	-0.502	-	-
2008-2014	0.013	-0.114	-0.401	-0.34	-0.457